REPORT

ORGANIC CHEMISTRY

A multifunctional catalyst that stereoselectively assembles prodrugs

Daniel A. DiRocco,* Yining Ji, Edward C. Sherer, Artis Klapars, Mikhail Reibarkh, James Dropinski, Rose Mathew, Peter Maligres, Alan M. Hyde, John Limanto, Andrew Brunskill, Rebecca T. Ruck, Louis-Charles Campeau, Ian W. Davies

The catalytic stereoselective synthesis of compounds with chiral phosphorus centers remains an unsolved problem. State-of-the-art methods rely on resolution or stoichiometric chiral auxiliaries. Phosphoramidate prodrugs are a critical component of pronucleotide (ProTide) therapies used in the treatment of viral disease and cancer. Here we describe the development of a catalytic stereoselective method for the installation of phosphorus-stereogenic phosphoramidates to nucleosides through a dynamic stereoselective process. Detailed mechanistic studies and computational modeling led to the rational design of a multifunctional catalyst that enables stereoselectivity as high as 99:1.

Almost half of antiviral and anticancer drugs currently on the market are nucleosides (*1*). Phosphorylation of the nucleoside in vivo is required for biological activity. However, nucleoside triphosphates are poor drug candidates, owing to their instability and ineffective transport across the cell membrane. The McGuigan ProTide (pronucleotide) platform markedly increases cell permeability and rate of in vivo phosphorylation by introduction of the 5′-aryloxy phosphoramidate moiety as a prodrug strategy (Fig. 1A) (*2*, *3*). The stereochemistry at phosphorus in the prodrug can substantially alter potency, rate of metabolism, and toxicity, making control of that stereocenter critical to a viable synthetic route. To date, standard methods for the stereoselective synthesis of P-stereogenic prodrugs have been limited to the use of chiral auxiliaries or chiral nonracemic phosphorylating agents, and critically, no general catalytic methods exist for their synthesis (Fig. 1A) (*4*–*8*).

The synthesis of carbon stereocenters is now the most mature subset in the field of asymmetric catalysis. Translation of these concepts to the synthesis of P-stereogenic compounds has remained an unmet synthetic need (*9*–*12*). Generation of phosphorus(V) heteroatom bonds in a catalytic and stereoselective manner would require either desymmetrization of an achiral species or a dynamic kinetic asymmetric transformation (DYKAT) that can stereoselect from an interconverting mixture of chiral P(V) intermediates (Fig. 1A) (*13*–*15*). Seminal reports of the formation of phosphoramidates via this strategy suffer from low catalytic turnover and poor stereoselectivity (*6*, *12*). Inherent to this problem is the lack of a canonical mechanism for P(V) bond formations, complicating the invention of a general protocol (*16*). In addition to stereoselectivity at phosphorus, a second crucial challenge associated with nucleoside phosphoramidation in ProTide synthesis and analogous applications is chemoselectivity for 5′ over 3′ phosphoramidation, resulting from indiscriminate activation of both hydroxyls. Enzymes have been shown to catalyze phosphorus-oxygen bond formation through a series of concomitant activation modes—including nucleophile activation by general base catalysis, leaving-group activation by general acid catalysis, and oxyanion hole–type stabilization of the transition state (Fig. 1B)—providing design principles for asymmetric catalysis (*17*, *18*). Here we report the design of a multifunctional catalyst that achieves high stereoselectivity at phosphorus in P–O bond-forming reactions.

We studied the reaction of chlorophosphoramidate **1** with nucleoside **2** to assemble a ProTide, MK-3682 (**3**) (Fig. 2), a hepatitis C virus (HCV) NS5b viral RNA polymerase inhibitor, currently in late-stage clinical trials for the treatment of HCV infection (*19*). A variety of achiral nucleophilic catalysts were examined to probe inherent substrate bias in the stereochemical outcome of the reaction. Under conditions originally reported by McGuigan [*N*-methyl imidazole (NMI), 2,6-lutidine], 49% yield of the desired phosphoramidated product was obtained, with a 52:48 (*R*):(*S*) ratio at the phosphorus center (Fig. 2A, entry 2). Given the lack of substantial stereochemical bias in either chiral substrate, we reasoned that stereoselectivity in this reaction could be fundamentally controlled by the catalyst. A survey of chiral nucleophilic catalysts demonstrated most to be ineffective at influencing the stereochemical outcome of the reaction; however, several analogs of the dihydropyrroloimidazole framework reported by Zhang and co-workers imparted promising levels of stereoselectivity at phosphorus (table S1) (*12*, *20*–*22*). Catalyst **(*R*)-A**, which contains a large *tert*-butyldimethylsilyl ether, facilitated the desired phosphoramidation in modest yield (60%) and 79:21 selectivity favoring the desired (*R*)-stereochemistry at phosphorus (Fig. 2A, entry 3). A mismatched relationship was observed using the opposite antipode of the catalyst (Fig. 2A, entry 4), suggesting chiral recognition of the nucleoside. This substrate-binding event was further corroborated by ^{1}H nuclear magnetic resonance (NMR) spectroscopy, with intermolecular nuclear Overhauser effects observed between these species (fig. S27). During further development, carbamates were identified as a privileged catalyst

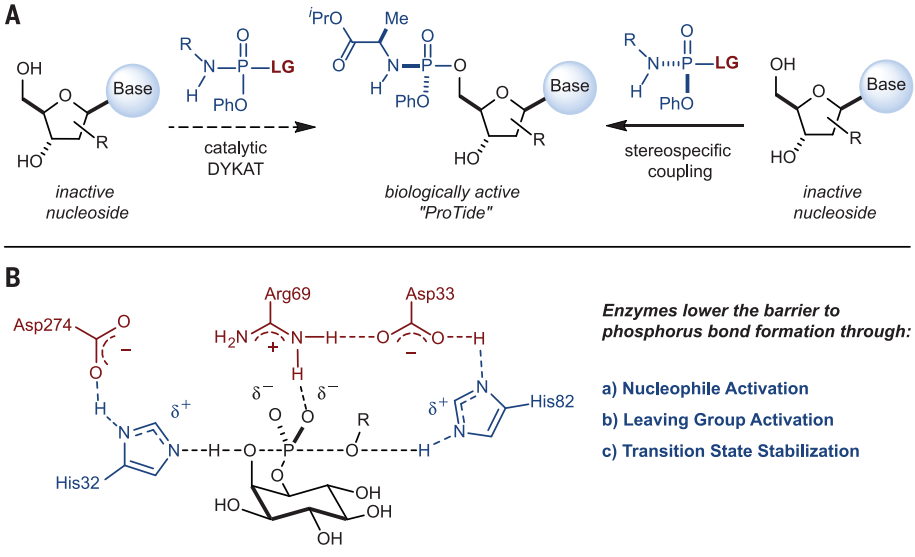

Fig. 1. Synthetic strategies and concepts for phosphorus-oxygen bond formation. (**A**) Approaches to the stereoselective synthesis of ProTides (pronucleotides). LG, leaving group; R, any atom; Ph, phenyl; ^{i}Pr, *iso*-propyl; DYKAT, dynamic kinetic asymmetric transformation. (**B**) Pentavalent transition state proposed by Ryan *et al*. (*17*) for P–O bond formation in phosphatidylinositol-specific phospholipase C.

Process Research and Development, Merck & Co., Inc., Rahway, NJ 07065, USA.
*Corresponding author. Email: daniel.dirocco@merck.com

motif. Catalyst (***R***)-**B** provided the product in moderate diastereoselectivity [89:11 diastereomeric ratio (d.r.) at 20 mol % loading] and excellent chemoselectivity for the 5′ hydroxyl (Fig. 2A, entry 7).

During optimization, we discovered the stereoselectivity of the reaction to be dependent on catalyst concentration, with higher selectivity observed at higher catalyst loadings (Fig. 2A, entries 7 to 9), consistent with a non–first-order catalytic pathway. Reaction progress kinetic analysis of temporal concentration profiles revealed a second-order dependence on catalyst concentration, first-order dependence on nucleoside, and saturation kinetics of 2,6-lutidine and chlorophosphoramidate **1** (figs. S3 to S6) (*23*, *24*). These data suggest that **1** is in rapid equilibrium with the activated species **4** and **5** and that P–O bond formation is the turnover-limiting step. The dynamic nature of the process was confirmed by ^{1}H and ^{31}P NMR spectroscopy, as no substantial change in the P-epimeric ratio of **1** was observed over the course of the reaction. Furthermore, exchange spectroscopy experiments unambiguously demonstrated that catalyst-mediated interconversion of phosphorylimidazolium chlorides **4** and **5** occurs rapidly under the reaction conditions, precluding a change in equilibrium as a source of stereocontrol (figs. S8 and S9).

Mechanistic studies of DMAP (4-dimethylaminopyridine)–catalyzed alcohol acylation have supported the hypothesis that the rate-determining step involves general base catalysis of the counteranion (*25*). We reasoned that a pathway reminiscent of an enzyme-mediated process involving concomitant activation of the phosphorus donor and general base catalysis of the 5′-hydroxyl could lead to the observed rate and selectivity enhancements. To test the validity of this hypothesis, we designed a chiral pyridine that was structurally analogous to catalyst **A** but was not sufficiently nucleophilic to activate chlorophosphoramidate **1**. When stereochemically matched pyridine (***R***)-**C** was used as a base in combination with catalyst (***R***)-**B**, an improvement in P stereoselectivity was observed with respect to the same experiment in

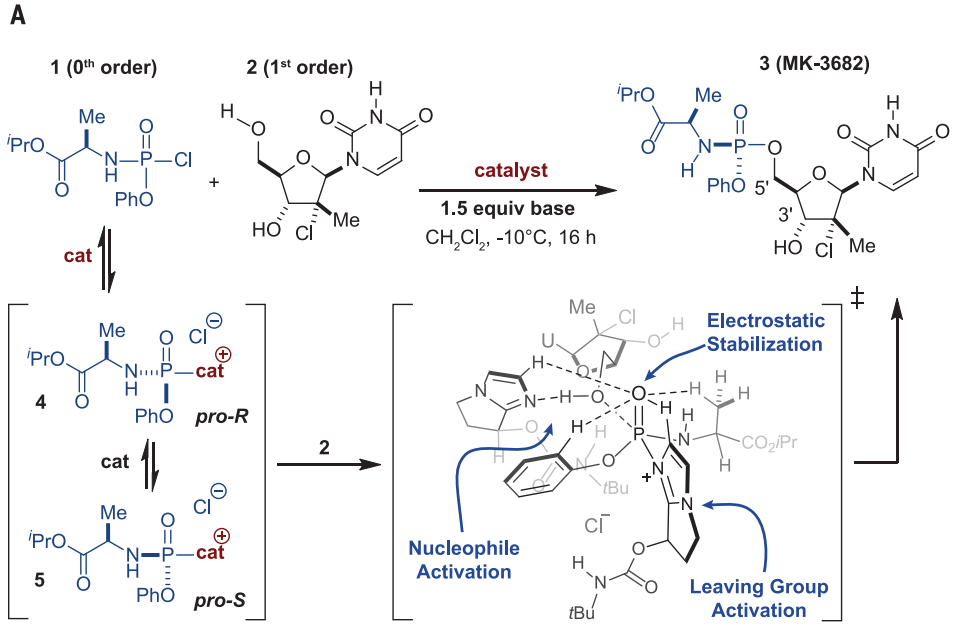

entry	mol % cat	base	5′:3′	% yield	P(*R*):P(*S*)
1	none	2,6-lutidine	ND	3	55:45
2	20% NMI	2,6-lutidine	96:4	49	52:48
3	20% (*R*)-A	2,6-lutidine	94:6	60	79:21
4	20% (*S*)-A	2,6-lutidine	94:6	47	44:56
5	5% (*R*)-B	2,6-lutidine	ND	12	71:29
6	10% (*R*)-B	2,6-lutidine	95:5	23	79:21
7	**20% (*R*)-B**	**2,6-lutidine**	**98:2**	**62**	**89:11**
8	40% (*R*)-B	2,6-lutidine	99:1	82	94:6
9	**100% (*R*)-B**	**none**	**99:1**	**60**	**96:4**
10	**20% (*R*)-B**	**(*R*)-C**	**98:2**	**44**	**93:7**
11	**20% (*R*)-B**	**(*S*)-C**	**98:2**	**47**	**74:26**
12	none	(*R*)-C	ND	5	74:26
13	none	(*S*)-C	ND	2	44:56

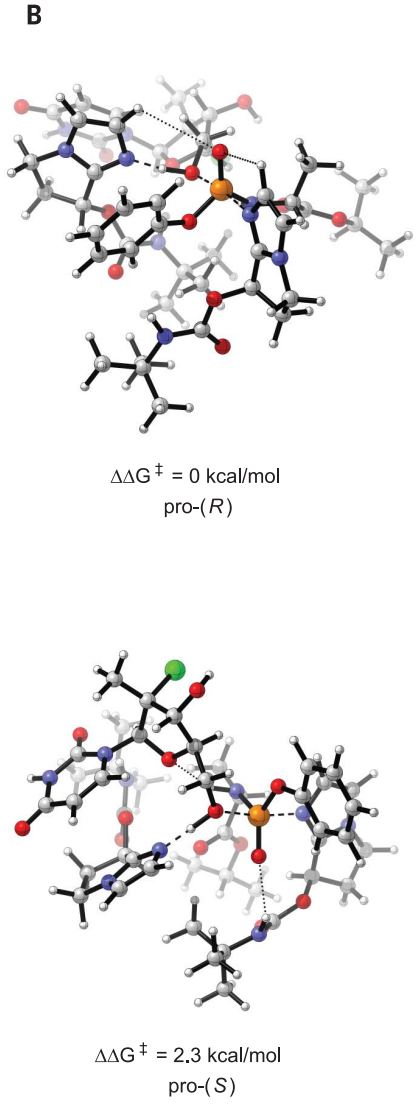

Fig. 2. Development of a stereoselective phosphoramidation. (**A**) Catalyst development and mechanistic study. Yield, P(*R*):P(*S*), and 5′:3′ ratios were determined by high-performance liquid chromatographic (HPLC) analysis. % yield refers to assay yield determined by HPLC analysis; 5′:3′ refers to the molar ratio of 5′- to 3′-hydroxyl phosphoramidation. Absolute stereochemistry of catalysts and relative stereochemistry of MK-3682 (**3**) was confirmed by single-crystal x-ray analysis (figs. S21 to S25). Cat, catalyst; Me, methyl; ^{t}Bu, *tert*-butyl; TBS, *tert*-butyldimethylsilyl; NMI, *N*-methyl imidazole; U, uracil; ND, not determined. (**B**) Transition state model of the second-order catalytic pathway. Calculations were performed at the M06L/6-31+G**//B3LYP-D3/6-31G** level of theory. Orange, phosphorus; red, oxygen; blue, nitrogen; green, chlorine; gray, carbon; white, hydrogen. $\Delta\Delta G^{\ddagger}$, relative free energy activation barrier.

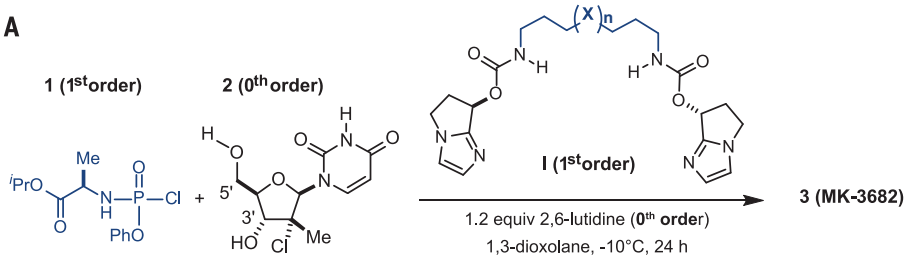

entry	cat	n=	X=	mol %	% 3'	% yield	d.r.
1	B	NA	NA	20	1.7	81.6	92:8
2	B	NA	NA	4	0.7	29.1	80:20
3	D	0	NA	2	1.0	76.3	88:12
4	E	1	CH_2	2	1.2	87.3	89:11
5	F	2	CH_2	2	0.6	90.3	97:3
6	G	3	CH_2	2	0.9	86.0	98:2
7	H	4	CH_2	2	2.3	85.0	98:2
8	**I**	**1**	***m*-C_6H_4**	**2**	**1.2**	**92.1**	**99:1**

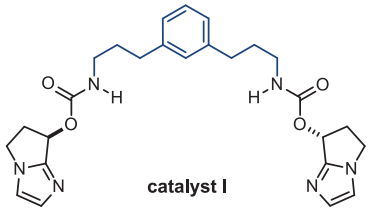

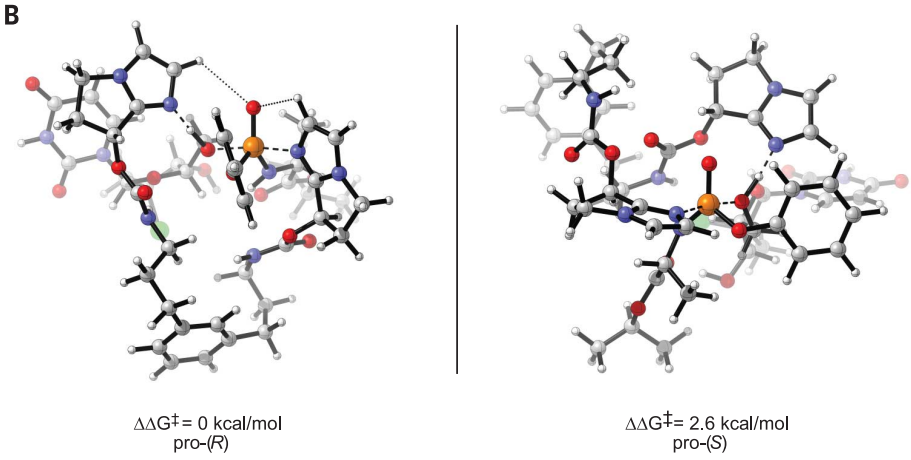

Fig. 3. Design of a dimeric phosphoramidation catalyst. (**A**) Linker optimization study. % yield, d.r., and % 3′ were determined by HPLC analysis. Yield refers to the combined yield of both 5′ diastereomers; d.r. refers to the P(*R*):P(*S*) ratio. n, number of units; NA, not applicable. (**B**) Transition state model of the stereoselective phosphorylation with dimeric catalyst **I**. Calculations were performed at the M06L/6-31+G**//B3LYP-D3/6-31G** level of theory.

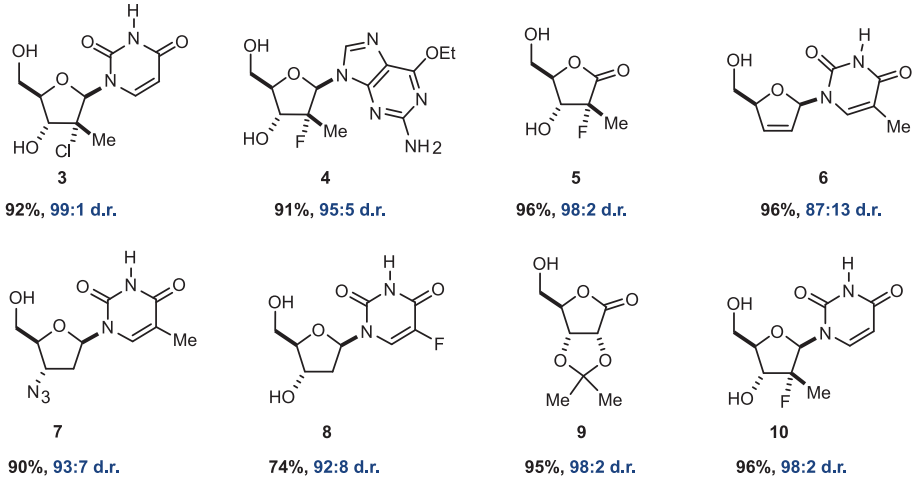

Fig. 4. Scope of the catalytic stereoselective phosphoramidation of nucleosides. Experiments were performed on a 100-mg scale (nucleoside) using 2 mol % catalyst **I**, 1.2 equivalents of **1**, and 1.2 equivalents of 2,6-lutidine in dioxolane at −10°C for 24 to 36 hours. Yield refers to combined assay yield of both 5′ diastereomers, as determined by ^{1}H NMR spectroscopy versus the internal standard. Diastereoselectivity (d.r.) refers to the P(*R*):P(*S*) ratio, as determined by ^{31}P NMR spectroscopy or HPLC analysis.

which 2,6-lutidine functioned as a base (Fig. 2A, entries 7 and 10). However, when stereochemically mismatched pyridine (***S*)-C** was employed, a marked loss of stereoselectivity was observed (Fig. 2A, entry 11). No substantial reaction occurs in the absence of catalyst (***R*)-B**, suggesting that both species are involved in the stereochemistry-determining event (*26*). Further evidence for a general base mechanism is provided by a positive kinetic isotope effect (k_H/k_D = 1.45, where k_H/k_D is the ratio of rate constants for hydrogen and deuterium, respectively), observed by deuteration of the 5′- and 3′-hydroxyl groups on the nucleoside.

To provide theoretical evidence for this distinctive activation mode, we examined our proposal by computational methods. Dispersion-corrected B3LYP/6-31G**, M06L/6-31+G**, and M06-2X/def2-TZVPP calculations in combination with a conformational sampling routine estimated the barrier of bond formation to be kinetically unfeasible (~30 kcal/mol) in the absence of a general base (tables S9 and S10) (*27*). In the presence of a second molecule of catalyst (***R*)-B**, a pentavalent transition state is characterized by a specific interaction in which the 5′-hydroxyl is hydrogen-bonded to the exogenous imidazole (Fig. 2B). This general base effect lowers the transition state energy by ~10 kcal/mol and thereby presents an accessible barrier to bond formation. Further interpretation of the transition state structures revealed a variety of interactions that stabilize the polarized P–O bond in the favored transition state (Fig. 2A). The preference for coplanarity of the imidazolium cation and the apical P–O bond results in a distinct CH–O interaction, facilitated by acidification of the α-C–H bond of the phosphorylated imidazole and bearing resemblance to the oxyanion hole in the catalytic triad of phospholipases (*17*, *18*, *28*). These systems share three common features: leaving group activation, general base catalysis, and oxyanion stabilization. Our method estimates these effects to provide a transition state differentiation of 2.3 kcal/mol, favoring the desired (*R*)-stereochemistry at phosphorus.

We hoped to develop a further-optimized catalyst that would reinforce these effects to achieve superior performance in both reaction rate and stereoselectivity. Inspired by the work of Jacobsen and co-workers, we envisioned a linking strategy that would increase cooperativity by reducing the entropic penalty of a highly ordered transition state (*29*, *30*). Our computational model suggested this strategy to be feasible, given the relative proximity of the respective carbamate side chains in the favored transition structure (Fig. 2B).

As a rational starting point for synthesis, a variety of carbamate linkages were modeled, suggesting the shortest feasible linkage between the two carbamate nitrogens to be six carbon atoms. Accordingly, dimers containing 6- to 10-carbon alkyl linkages were synthesized and compared with catalyst (***R*)-B** under identical reaction conditions (Fig. 3A). The shorter linkages (six or seven carbons) provided a substantial improvement in efficiency while only modestly increasing selectivity with respect to catalyst (***R*)-B** at similar loading (Fig. 3A, entries 3 and 4). A profound effect was

observed at eight atoms (catalyst **F**), providing the desired phosphoramidate in 90% yield and 97:3 d.r. and validating our computationally driven design principle (Fig. 3A, entry 5). Maximum selectivity was achieved at nine atoms (catalyst **G**, 98:2 d.r.); further lengthening of the linker resulted in erosion of both stereoselectivity and chemoselectivity, likely on account of undesirable flexibility. Given this observation, we anticipated that further conformational restriction of the linker would result in increased selectivity through the reduction of rotational degrees of freedom. As such, catalyst **I**, which contains a central 1,3-phenyl group, was synthesized and displayed optimal reactivity [relative rate k_{rel} = 10 versus (***R***)-**B** (fig. S16)] and further improved stereoselectivity (99:1 d.r.).

To better understand the effect of catalyst linkage on stereoselectivity, we reoptimized the transition states with linked catalyst **I** (Fig. 3B). Relative transition state energies predict the desired P-(*R*) stereochemistry to be favored by 2.6 kcal/mol, in agreement with the higher experimentally observed selectivity (*31*). The same structural preferences are conserved and further amplified in this structure (table S15).

Experimental validation of intramolecular cooperativity was garnered by the observation of a change to first-order dependence on catalyst concentration in this system (fig. S14). We were initially concerned that linking catalysts might result in deactivation through competitive bisphosphoramidation of the dimer. Surprisingly, P–O bond formation proved considerably faster than chlorophosphoramidate activation, exemplified by first- and zero-order kinetics of chlorophosphoramidate **1** and nucleoside **2**, respectively (figs. S11 and S12). These data suggest a change in the turnover-limiting step to chlorophosphoramidate activation. Given that P–O bond formation is faster than activation of **1**, it seemed plausible that equilibration may be a stereo-determining factor in this system. However, ^{31}P NMR studies revealed a single observable species, consistent with fast equilibration and a lower barrier to P inversion through a cooperative displacement mechanism (figs. S32 and S33). As argued by Albery and Knowles in their view of the "evolutionary perfection" of an enzyme, the enzyme must confront the problem of finding a mechanism that lowers the barrier to each elementary step (*32*). We have demonstrated that this catalyst lowers barriers to P–O bond formation and P(V) inversion but is turnover-limited by the rate of catalyst addition to **1**. Arguably, further development could address this shortcoming, closing the gap to "evolutionary perfection."

Although this catalyst was optimized for use in a single ProTide therapeutic (MK-3682), the key principles that govern selectivity proved generally applicable to other nucleoside analogs. A variety of ribofuranose-based nucleosides could be phosphorylated with high P stereoselectivity by means of this method (Fig. 4). Neither the nucleobase nor the C3′ hydroxyl is an important driver for selectivity, exemplified in the highly stereoselective phosphoramidation of dihydrofuranones **5** and **9**. Deoxyribofuranose derivatives, lacking a C2′ substituent, are tolerated; notably, the anti-HIV nucleoside derivative azidothymidine (AZT) (**7**) could be converted to the prodrug in 93:7 d.r. In a seminal paper, McGuigan *et al*. reported this nucleoside to yield only a 2:1 mixture of diastereomers when phosphoramidated in the presence of NMI (*33*).

Through a distinctive activation mode, we have designed a practical small-molecule catalyst that mimics the complex function of an enzyme, culminating in phosphoramidation that is highly stereoselective at the phosphorus center. The general applicability of the catalyst to a broad range of therapeutically relevant nucleophiles invites its rapid adoption in the preparation of these clinically important molecules.

REFERENCES AND NOTES

1. L. P. Jordheim, D. Durantel, F. Zoulim, C. Dumontet, *Nat. Rev. Drug Discov.* **12**, 447–464 (2013).
2. D. Cahard, C. McGuigan, J. Balzarini, *Mini Rev. Med. Chem.* **4**, 371–381 (2004).
3. M. J. Sofia *et al*., *J. Med. Chem.* **53**, 7202–7218 (2010).
4. U. Pradere, E. C. Garnier-Amblard, S. J. Coats, F. Amblard, R. F. Schinazi, *Chem. Rev.* **114**, 9154–9218 (2014).
5. B. S. Ross, P. G. Reddy, H.-R. Zhang, S. Rachakonda, M. J. Sofia, *J. Org. Chem.* **76**, 8311–8319 (2011).
6. F. Pertusati, C. McGuigan, *Chem. Commun.* **51**, 8070–8073 (2015).
7. K. Tran *et al*., *J. Org. Chem.* **80**, 4994–5003 (2015).
8. J. M. McCabe Dunn *et al*., *Chem. Sci.* **8**, 2804–2810 (2017).
9. B. R. Sculimbrene, S. J. Miller, *J. Am. Chem. Soc.* **123**, 10125–10126 (2001).
10. C. M. Longo, Y. Wei, M. F. Roberts, S. J. Miller, *Angew. Chem. Int. Ed.* **48**, 4158–4161 (2009).
11. J. W. Evans, M. B. Fierman, S. J. Miller, J. A. Ellman, *J. Am. Chem. Soc.* **126**, 8134–8135 (2004).
12. S. Liu *et al*., *Tetrahedron Asymmetry* **23**, 329–332 (2012).
13. J. Steinreiber, K. Faber, H. Griengl, *Chem. Eur. J.* **14**, 8060–8072 (2008).
14. W. B. Farnham, R. A. Lewis, R. K. Murray Jr., K. Mislow, *J. Am. Chem. Soc.* **92**, 5808–5809 (1970).
15. M. Dutartre, J. Bayardon, S. Jugé, *Chem. Soc. Rev.* **45**, 5771–5794 (2016).
16. C. Brown, J. A. Boudreau, B. Hewitson, R. F. Hudson, *J. Chem. Soc. Chem. Commun.* **1975**, 504–505 (1975).
17. M. Ryan, T. Liu, F. W. Dahlquist, O. H. Griffith, *Biochemistry* **40**, 9743–9750 (2001).
18. L.-C. Lee, Y.-L. Lee, R.-J. Leu, J.-F. Shaw, *Biochem. J.* **397**, 69–76 (2006).
19. Merck Sharp & Dohme Corp., Efficacy and Safety of grazoprevir (MK-5172) and MK-3682 with elbasvir (MK-8742) or ruzasvir (MK-8408) for chronic hepatitis C virus (HCV) genotype (GT) 3, GT4, GT5, and GT6 Infection (MK-3682-012). in ClinicalTrials.gov. [Internet] Bethesda (MD): National Library of Medicine (US). 2000- [cited 21 November 2016]. Available from: https://clinicaltrials.gov/ct2/show/NCT02332720; NLM Identifier NCT02332720.
20. P. M. Weintraub, P. L. Tiernan, J. C. Huffman, *J. Het. Chem.* **24**, 561–563 (1987).
21. Z. Zhang, F. Xie, J. Jia, W. Zhang, *J. Am. Chem. Soc.* **132**, 15939–15941 (2010).
22. A. S. De Miranda *et al*., *J. Mol. Catal. B* **91**, 77–80 (2013).
23. D. G. Blackmond, *Angew. Chem. Int. Ed.* **44**, 4302–4320 (2005).
24. The less-selective catalyst (***R***)-**A**, based on the same bicyclic framework but lacking the carbamate functionality, exhibited a first-order dependence (fig. S10).
25. S. Xu *et al*., *Chemistry* **11**, 4751–4757 (2005).
26. A traditional nonlinear-effect study was not meaningful in this case because of the diastereomeric relationship of the products and the complex equilibria associated with the chiral reactants.
27. Owing to the complexity in sampling van der Waals precomplexes, we report relative activation free energies in relation to a common interconverting lowest-energy species.
28. Estimates of the pK_a (where K_a is the acid dissociation constant) of this C–H moiety suggest that it is more acidic than an amide or imidazole N–H, frequently implicated in oxyanion hole–type stabilization.
29. R. G. Konsler, J. Karl, E. N. Jacobsen, *J. Am. Chem. Soc.* **120**, 10780–10781 (1998).
30. S. E. Denmark, S. K. Ghosh, *Angew. Chem. Int. Ed.* **40**, 4759–4762 (2001).
31. The experimentally determined selectivities for catalysts **B** and **I** correspond to energy differences at 263 K of 1.66 and 2.40 kcal/mol, respectively.
32. W. J. Albery, J. R. Knowles, *Biochemistry* **15**, 5631–5640 (1976).
33. C. McGuigan, R. N. Pathirana, N. Mahmood, A. J. Hay, *Bioorg. Med. Chem. Lett.* **2**, 701–704 (1992).

ACKNOWLEDGMENTS

We thank Y. Yu for synthesis of catalyst libraries, J. Liu and M. Biba for separations support, Y. Liu for NMR support, J. Forbes and H. Gurukar for high-performance computing support, and E. N. Jacobsen for helpful discussions. Structural parameters for compounds **3**, (***R***)-**B**, (***R***)-**J**, and (***R***)-**G** are available free of charge from the Cambridge Crystallographic Data Centre under accession numbers CCDC-1525797, CCDC-1523526, CCDC-1523527, and CCDC-1523528, respectively. Full details of the kinetic, spectroscopic, and computational studies are available in the supplementary materials. Stationary points for all computed structures can be located in data S1.

SUPPLEMENTARY MATERIALS

www.sciencemag.org/content/356/6336/426/suppl/DC1
Materials and Methods
Figs. S1 to S41
Tables S1 to S17
References (*34*–*63*)
NMR Spectra
Data S1

17 January 2017; accepted 9 March 2017
10.1126/science.aam7936

A multifunctional catalyst that stereoselectively assembles prodrugs

Daniel A. DiRocco, Yining Ji, Edward C. Sherer, Artis Klapars, Mikhail Reibarkh, James Dropinski, Rose Mathew, Peter Maligres, Alan M. Hyde, John Limanto, Andrew Brunskill, Rebecca T. Ruck, Louis-Charles Campeau and Ian W. Davies (April 27, 2017)
Science **356** (6336), 426-430. [doi: 10.1126/science.aam7936]

Editor's Summary

Getting phosphorus into healthy shape

ProTide therapeutics play a trick on the body, getting nucleoside analogs where they need to be by decorating them with unnatural phosphoramidates in place of ordinary phosphates. These compounds pose an unusual synthetic challenge because their configuration must be controlled at phosphorus; most methods have been refined to manipulate the geometry of carbon. DiRocco *et al.* report a metal-free, small-molecule catalyst that attains high selectivity for nucleoside phosphoramidation by activating both reaction partners. Kinetic studies with an early prototype revealed a double role for the catalyst that inspired the rational design of a more active and selective dimeric structure.

Science, this issue p. 426

Science (print ISSN 0036-8075; online ISSN 1095-9203) is published weekly, except the last week in December, by the American Association for the Advancement of Science, 1200 New York Avenue NW, Washington, DC 20005.